Journal of Pathology
J Pathol 2017; **241:** 350–361
Published online 29 December 2016 in Wiley Online Library (wileyonlinelibrary.com) DOI: 10.1002/path.4841

ORIGINAL PAPER

Functional and prognostic significance of the genomic amplification of frizzled 6 (*FZD6*) in breast cancer

Gabriele Corda,[1,2] Gianluca Sala,[3,4] Rossano Lattanzio,[4] Manuela Iezzi,[5] Michele Sallese,[4,6] Giorgia Fragassi,[4,6] Alessia Lamolinara,[5] Hasan Mirza,[7] Daniela Barcaroli,[8] Sibylle Ermler,[1,2] Elisabete Silva,[1,2] Hemad Yasaei,[1] Robert F Newbold,[1,2] Paola Vagnarelli,[1,2] Marcella Mottolese,[9] Pier Giorgio Natali,[3] Letizia Perracchio,[9] Jelmar Quist,[7] Anita Grigoriadis,[7] Pierfrancesco Marra,[7] Andrew N Tutt,[7,10] Mauro Piantelli,[4] Stefano Iacobelli,[3,4] Vincenzo De Laurenzi[4]* and Arturo Sala[1,2,8]*

[1] *College of Health and Life Sciences, Brunel University London, Uxbridge, UK*
[2] *Institute of Environment, Health and Societies, Brunel University London, Uxbridge, UK*
[3] *MediaPharma srl, Chieti, Italy*
[4] *Dipartimento di Scienze Mediche, Orali e Biotecnologiche, CESI-MeT, University G. D'Annunzio, Chieti, Italy*
[5] *Dipartimento di Medicina e Scienze dell'Invecchiamento, CESI-MeT, University G. D'Annunzio, Chieti, Italy*
[6] *Fondazione Mario Negri Sud, S. Maria Imbaro, Italy*
[7] *Breast Cancer Now Unit, Research Oncology, King's Health Partners AHSC, Faculty of Life Sciences and Medicine, King's College London, London, UK*
[8] *Dipartimento di Scienze Psicologiche, della Salute e del Territorio, CESI-MeT, University G. D'Annunzio, Chieti, Italy*
[9] *Regina Elena Cancer Institute, Rome, Italy*
[10] *Breast Cancer Now, The Institute of Cancer Research, London, UK*

**Correspondence to: A Sala, Institute of Environment, Health and Societies, College of Health and Life Sciences, Heinz Wolff Building, Brunel University London, UB8 3PH Uxbridge, UK. E-mail: arturo.sala@brunel.ac.uk*
Or VD Laurenzi, Dipartimento di Scienze Mediche, Orali e Biotecnologiche, CESI-MeT, University G. D'Annunzio, Chieti, 66100, Italy. E-mail: delaurenzi@unich.it

Abstract

Frizzled receptors mediate Wnt ligand signalling, which is crucially involved in regulating tissue development and differentiation, and is often deregulated in cancer. In this study, we found that the gene encoding the Wnt receptor frizzled 6 (*FZD6*) is frequently amplified in breast cancer, with an increased incidence in the triple-negative breast cancer (TNBC) subtype. Ablation of *FZD6* expression in mammary cancer cell lines: (1) inhibited motility and invasion; (2) induced a more symmetrical shape of organoid three-dimensional cultures; and (3) inhibited bone and liver metastasis *in vivo*. Mechanistically, FZD6 signalling is required for the assembly of the fibronectin matrix, interfering with the organization of the actin cytoskeleton. Ectopic delivery of fibronectin in FZD6-depleted, triple-negative MDA-MB-231 cells rearranged the actin cytoskeleton and restored epidermal growth factor-mediated invasion. In patients with localized, lymph node-negative (early) breast cancer, positivity of tumour cells for FZD6 protein identified patients with reduced distant relapse-free survival. Multivariate analysis indicated an independent prognostic significance of *FZD6* expression in TNBC tumours, predicting distant, but not local, relapse. We conclude that the FZD6–fibronectin actin axis identified in our study could be exploited for drug development in highly metastatic forms of breast cancer, such as TNBC.

Keywords: Wnt signalling; metastasis; xenograft; mouse model; actin cytoskeleton

Received 9 March 2016; Revised 9 September 2016; Accepted 18 October 2016

No conflicts of interest were declared.

Introduction

Breast cancer is the most frequent malignancy in women, accounting for >200 000 new cases per year in the USA and 350 000 in Europe [1–3]. A decline in the mortality resulting from breast cancer has recently been documented, most likely as the result of the combination of an increase in public awareness, the implementation of screening programnes, and advances in adjuvant treatments [1,3]. Screening programmes have increased the detection of early-stage, node-negative tumours with a low risk of recurrence. Approximately 70–80% of these patients are cured by local or regional treatment, often in combination with adjuvant systemic therapy, which significantly reduces the risk of recurrence [4]. Risk-group discrimination is achieved by assessing prognostic factors, such as tumour size and grade, hormone receptor status, age, or menopausal

status. Despite the majority of patients without nodal involvement receiving some form of adjuvant treatment, approximately one-third will experience recurrence [5,6].

The Wnt pathway is an important regulator of tissue development in different organ systems [7–9]. There are 10 Wnt receptors in mammalian cells; called frizzled (e.g. FZD1–FZD10), they activate a canonical or a non-canonical pathway, depending on the ligand and the cell type. Frizzled receptors, including FZD7, FZD3, and FZD2, and Wnt ligands, such as WNT3a and WNT5a/b, have been shown to play an important role in promoting aggressive behaviour, instigating the growth of breast cancer cells [10–13] and cancer stem cells in the metastatic niche [10]. The possible involvement of FZD6 in transformation is emerging, because this receptor is overexpressed in several cancers, including hepatocarcinoma, colon cancer, prostate cancer, and leukaemia [14–17]. Our own group has revealed that *FZD6* expression is associated with drug resistance and increased invasiveness in neuroblastoma, marking cancer-initiating cells [18]. In the present study, we examined whether FZD6 activity is required for breast cancer cell growth, motility and metastasis *in vitro* and *in vivo*.

Materials and methods

Patients and tissues

The study included 352 primary infiltrating breast cancers from N0 and T1/T2 tumours, diagnosed between 1985 and 2003 at the Regina Elena National Cancer Institute, Rome, Italy, and presenting primary unilateral breast carcinoma. The study was reviewed and approved by the ethics committee of the Regina Elena National Cancer Institute, and written informed consent was obtained from all patients. Patient and tumour characteristics are summarized in supplementary material, Table S1. All patients received radiation therapy, 138 patients received hormonal therapy and 140 patients were treated with adjuvant chemotherapy (followed or not by hormonal therapy) and are members of the oestrogen-receptor (ER)-positive cohort. Patients with HER2-positive tumours did not receive trastuzumab, because it was not used in breast tumour therapy in the study period. Follow-up data were obtained from institutional records or by the referring physicians. The median follow-up was 80 months (range 6–298 months). During follow-up, 32 patients (9.1%) developed a local recurrence, and distant metastases were observed in 54 cases (15.3%).

Cell culture

The cell lines used were kindly provided by P. Marra [King's College London (KCL)] and R.F. Newbold (Brunel University): BT474 – luminal-like metastatic ductal carcinoma; MDA-MB-231 – basal-like metastatic adenocarcinoma; MDA-MB-436 – basal-like adenocarcinoma; HCC1143 – basal-like ductal carcinoma; HEK FT293 - human embryonic kidney cells; MCF7 – luminal-like metastatic adenocarcinoma; SK-BR-3 – basal-like adenocarcinoma; T47D –ductal adenocarcinoma; and BT20 – basal-like adenocarcinoma. All cell lines had been independently validated by short tandem repeat genotyping. MDA-MB-231, HCC1143 and MDA-MD-436 cells were grown in RPMI medium (Sigma Aldrich, St Louis, MO, USA) 1 mM in sodium pyruvate (Gibco, ThermoFisher Scientific, Pittsburgh, PA, USA), supplemented with 10% fetal bovine serum (FBS) (Gibco). HEK-FT293, MCF7 and SK-BR-3 cells were grown in Dulbecco's modified Eagle's medium (DMEM) (Sigma) 1 mM in sodium pyruvate, supplemented with 10% FBS. BT20 and BT474 cells were grown in a mixture of 50% DMEM and 50% Ham's F12, supplemented with 10% FBS. Cells were maintained at 37 °C in a humidified atmosphere with 5% CO_2. Human mammary epithelial cells (HMECs) were cultured as described previously [19].

MTS assay

The reagent 3-(4,5-dimethylthiazol-2-yl)-5-(3-carboxymethoxyphenyl)-2-(4-sulfophenyl)-2H-tetrazolium (MTS) (Promega, Madison, WI, USA) was added to cell cultures in 96-well plates, and then incubated at 37 °C for 2–4 h before reading of the absorbance at 490 nm with a plate reader (Bio-Rad, Hercules, CA, USA).

Cell invasion assay

Between 30 000 and 180 000 cells were seeded in 500 µl of medium without serum, and placed in the upper chamber of Matrigel-coated invasion chambers (Becton Dickinson, Franklin Lakes, NJ, USA). After 22 h, the membrane was removed from the insert with a scalpel, stained with crystal violet, and placed on a glass slide. Pictures of the membrane were taken with a camera connected to a microscope (Zeiss axioscope 2, Oberkochen, Germany), and the number of cells invading the Matrigel was determined with ImageJ software.

Plasmid construction

RNA was extracted from MDA-MB-231 cells, and reverse-transcribed with an RNA-to-cDNA Kit (Applied Biosystems, Foster City, CA, USA). The FZD6 cDNA was polymerase chain reaction (PCR)-amplified with the primers CGCGGGTACCAGGAATTTGAAGAA AATGGAAATG (forward) and GCGATCTAGAGT TCTTCAAGTATCTGAATGACAACC (reverse), containing a *Kpn*1 and an *Xba*1 restriction site, respectively. The PCR product was cut with *Kpn*1 and *Xba*1 restriction enzymes, and cloned into the expression vector pcDNA3.1 (Invitrogen, Carlsbad, CA, USA).

Cell motility assay

Cells (3.8×10^5) were seeded into bipartite chambers for live imaging (Fisher, Hampton, NH, USA), and

allowed to grow for 24 h in 1 ml of complete medium. The medium was then replaced with 2 ml of Leibovitz's L-15 medium (Gibco), and the cells were placed back in the incubator for 4 h. The cell monolayers were then wounded with a sterile pipette tip and placed in a live imaging microscope (Nikon Eclipse Ti, Tokyo, JP). At least four different areas of each wound were photographed every 30 min for 24 h. Cell trajectories were tracked and path lengths measured over a period of 16 h with the image analysis software NIS-Elements (Nikon). The average speed of a minimum of 10 cells was scored in four areas of each wound analysed.

Orthotopic transplantations in immunodeficient mice

NOD *scid* gamma (NSG) mice were purchased from the Jackson Laboratory, Bar Harbour, ME, USA, and bred in the animal facility of Aging Research Centre, G. D'Annunzio University, Chieti. Animal care and experimental procedures were approved by the Ethics Committee for Animal Experimentation of the institute, according to the Italian law. Eight-week-old female mice (10 mice per group) were injected unilaterally with 3.5×10^6 cells into the fourth mammary fat pad. Tumour growth was monitored biweekly with callipers up to 96 days or until tumours reached 0.3 cm^3 in volume. Tumour volume was calculated as $0.5 \times d1^2 \times d2$, where d1 and d2 are the smaller and larger diameters, respectively. Primary tumours and organs were fixed in 10% neutral buffered formalin, paraffin-embedded, sectioned, and stained with haematoxylin and eosin (H&E). Slides were evaluated independently by two pathologists. To quantify microscopic metastases, livers were cut transversally into 2.0-mm-thick parallel slabs starting from a random position, resulting in 8–10 slabs. Semiquantitative evaluation was performed, with each sample being attributed a value from 1 to 4, based on the number and size of metastases; 1 was attributed to organs with a few small metastases, and 4 to organs with numerous large metastases. Fisher's exact test was used to compare differences in metastatic spread.

Glutathione-*S*-transferase (GST) pull-down and western blot analysis

Western blot analysis was carried out as described previously [18]. Total active Rho was quantified with a pull-down/western blotting detection kit, according to the manufacturer's instructions (Thermofisher, Pittsburgh, PA, USA). The primary antibodies used were: anti-FZD6 (D16E5; dilution 1:1000; Cell Signaling, Boston, MA); anti-β-actin (I-19; dilution 1:1000; Santa Cruz, Dallas, TX, USA); and anti-glyceraldehyde-3-phosphate dehydrogenase (AB8245; dilution 1:1000; Abcam, Cambridge, UK).

Bioinformatic analysis

R version 3.1.0 (2014-04-10) was used for all analyses and diagrammatic representation of data. Gene ontology (GO) enrichment was performed with ConsensusPathDB-human enrichment tools [20,21], and a dendrogram was created with QuickGO [22]. All *p*-values reported in boxplots were determined with a two-sided Wilcoxon rank sum test, and adjusted for multiple testing by use of the false discovery rate [23].

Reverse transcription quantitative PCR (RT-qPCR

Total cellular RNA was extracted and reverse-transcribed as described previously [24].

KCL and Molecular Taxonomy of Breast Cancer International Consortium (METABRIC) data

A detailed description of the KCL data and METABRIC data, such as sample demographics and bioinformatics analyses, has been published previously [25–27]. A diagram depicting the studies from which the samples of the KCL cohort used in this study were derived is shown in supplementary material, Figure S1.

Immunohistochemistry

Tissue microarrays were constructed by extracting 2-mm-diameter cores of histologically confirmed invasive breast carcinoma areas, as previously described [28]. After antigen retrieval (microwave treatment at 750 W for 10 min in 10 mM sodium citrate buffer, pH 6.0), 5-μm sections were incubated overnight at 4 °C with the anti-FZD6 antibody (Novus Biological, Littleton, CO, USA) at 1:100 dilution. The anti-rabbit EnVision kit (K4003; Dako, Glostrup, Denmark) was used for signal amplification. In control sections, the specific primary antibody was replaced with non-immune serum. Seventy-one of 352 (20.2%) cases showed positive staining for FZD6, and the percentages of tumour cells positive in each sample ranged from 2 to 85% [mean: 23.8 ± 2.5 standard error (SE)]. Positivity for FZD6 in each subtype was as follows: luminal A-like, 21.1%; luminal B-like (HER2-negative), 22.0%; luminal B-like (HER2-positive), 15.2%; HER2 positive (non-luminal), 23.8%; and triple-negative (ductal), 14.9%. The following antibodies were used for the identification of tumour subtypes, as previously reported [29]: the anti-ER-α monoclonal antibody (mAb) 6F11 (1:50; Novocastra, Leica Biosystems, Newcastle upon Tyne, UK), the anti-progesterone receptor (PgR) mAb 1A6 (1:40; Novocastra, Leica Biosystems), and the anti-Ki67 mAb MIB-1 (1:75; Dako, Ely, UK). HER2 was detected with the Herceptest kit, and the slides were stained according to the manufacturer's instructions (Dako, Ely, UK). Immunohistochemical analysis was performed by two pathologists (M.P. and R.L.) by consensus, without knowledge of the clinicopathological information.

ER, PgR and Ki67 expression were dichotomized according to the St Gallen criteria [30]. HER2 membranous staining was scored with the Herceptest kit, and classified as positive if the intensity was scored as 3+, with ?30% of cells showing complete membrane

staining [31]. The relationships between FZD6 expression and clinicopathological parameters were assessed with Pearson's χ^2 or Fisher's exact test, as appropriate. Kaplan–Meier plots were used to illustrate the survival in specified cohorts, and the log-rank test was used to test for equality of survival curves. The association of FZD6 expression with outcome, adjusted for other prognostic factors, was tested by multivariate analysis (Cox's proportional hazards model). The following covariates were included in the multivariate disease-free survival (DFS) models: tumour size and grade, and ER, PgR, Ki67, HER2 and FZD6 status. Appropriateness of the proportional hazard assumption was assessed by plotting the log cumulative hazard functions over time and checking for parallelism. SPSS Version 15.0 (SPSS, Chicago, IL, USA) was used throughout, and $p < 0.05$ was considered to be statistically significant.

Results

FZD6 is frequently amplified and overexpressed in triple-negative breast cancer (TNBC)

Given the importance of Wnt signalling in breast cancer, we systematically analysed gene copy number variations (CNVs) and expression of the 10 known Wnt receptor genes (*FZD1* to *FZD10*) in the Sanger Institute Cosmic repository [32]. Frizzled receptor genes are only marginally altered in breast cancer as compared with normal tissue, with the exception of *FZD6*. Indeed, 19.11% of breast samples showed *FZD6* copy number gains and 18.71% gene overexpression quantified as *z*-score (supplementary material, Table S2). In comparison, *FZD7* and *FZD2*, which have been previously implicated in aggressive breast cancer [12,13], were overexpressed only in 4% of tumours, without copy number gains (supplementary material, Table S2). Bioinformatic analysis with the METABRIC database [33] indicated that *FZD6* is amplified or gained in 73.2% of breast cancers (supplementary material, Figure S2A). Notably, *FZD6* copy number increase was more frequent in triple-negative (87.1%) than in ER-positive (72%) cases (χ^2 11.0493; $p = 0.000887$). Increased expression levels of *FZD6* were particularly observed in tumour samples containing the amplification, suggesting that this could drive gene expression in some breast carcinomas (supplementary material, Figure S2A). To corroborate these findings, we assessed the gene expression and copy number data from a primary breast cancer cohort enriched for triple-negative cases collected at KCL (supplementary material, Figure S1) [25,27]. The KCL cohort confirmed that *FZD6* CNVs were common in breast cancer (81.1% cases with gains or amplification) and that there was an increased incidence of *FZD6* copy number gain and amplification in triple-negative (88.1%) as compared with non-triple-negative (61.7%) (χ^2 13.7129; $p = 0.000213$) or HER2-positive (63.1%) (χ^2 6.9591, $p = 0.0083$) cases, explaining the increased gene expression in this subtype (Figure 1A–C; supplementary material, Figure S2B). Expression of the non-canonical FZD6 ligands WNT11 and WNT5B, but not of the canonical WNT1 and WNT3A, was also increased in triple-negative samples as compared with other subtypes, suggesting that a Wnt non-canonical signalling axis could be activated downstream of *FZD6* in aggressive forms of breast cancer (Figure 1D–G). Overall, the bioinformatic analyses and our previous study, in which we demonstrated that FZD6 promotes metastasis and a stem cell-like phenotype in neuroblastoma [18], prompted us to further investigate the role of this receptor in the aggressive behaviour of mammary cancer cells.

FZD6 regulates motility, invasion and three-dimensional (3D) growth, but not proliferation, of breast cancer cell lines

To assess *FZD6* expression in breast cancer cell lines, we prepared total cellular RNAs and protein lysates from a panel of breast cancer cell lines representative of the different molecular subtypes. Normal HMECs and their hTERT-immortalized counterparts were also used for comparison. RT-qPCR and ImageStream analyses show that expression of *FZD6* was higher in immortalized HMECs than in normal human epithelial cells (supplementary material, Figure S3A, C). Among breast cancer cell lines, basal-like cells generally expressed more FZD6 than luminal ones, although the samples were too small to determine statistical significance. This trend corroborates the hypothesis that frequent *FZD6* amplification in basal cells might induce high levels of FZD6 expression. The difference in protein expression was not, however, reflected at the RNA level (supplementary material, Figure S3A, B). We next assessed the expression of FZD6 on cell surfaces by using flow cytometry and ImageStream analysis. With the exception of MB-MDA-436, all breast cancer cell lines expressed FZD6 on the plasma membrane, although the mean fluorescence intensity and percentage of positive cells varied among the different samples (supplementary material, Figure S3D, E).

To study the physiological role of FZD6 in breast cancer, we investigated its role in cell motility, as non-canonical Wnt signalling is known to regulate this cell function. First, we ectopically overexpressed a FZD6 cDNA into luminal SK-BR-3 and T47D cells, in which expression of FZD6 protein is low (supplementary material, Figure S3B; Figure 2A). Live cell imaging indicated that overexpression of FZD6 caused a significant increase in SK-BR-3 and T47D cell motility (Figure 2B). Accordingly, depletion of endogenous FZD6 with short-hairpin RNAs (shRNAs) significantly reduced motility of FZD6^{high} triple-negative MDA-MB-231 cells in wound healing assays (Figure 2C). Verification of FZD6 mRNA and protein depletion is shown in supplementary material, Figure S4A.

We next assessed the role of FZD6 in the proliferation and invasion of breast cancer cell lines by using transient

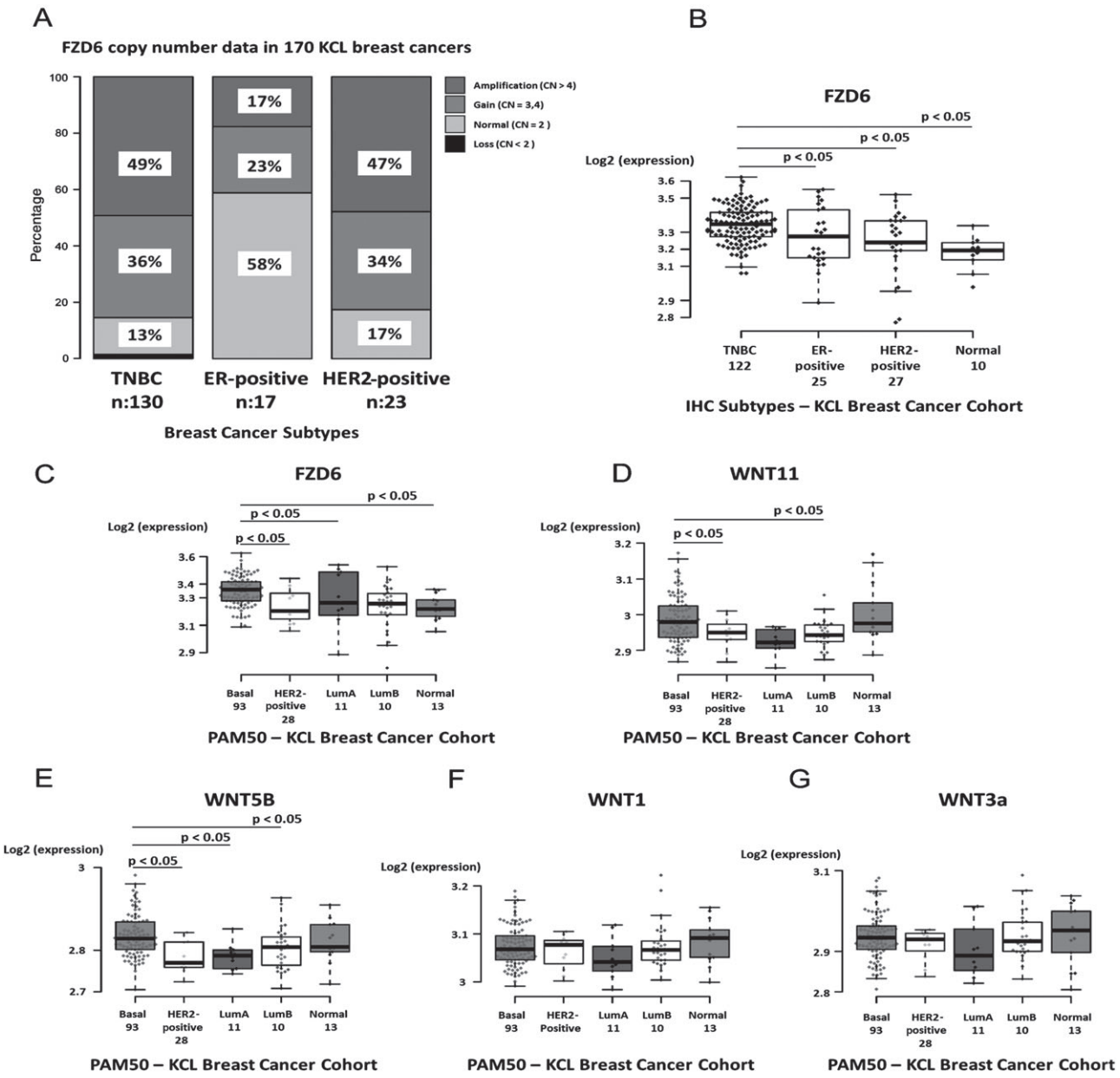

Figure 1. Analysis of CNV and expression of the *FZD6* and *WNT* genes in breast cancer samples from KCL data. (A) Distribution of CNVs, as defined by ASCAT (http://www.pnas.org/content/107/39/16910.long), of *FZD6* in breast cancer subtypes defined according to immunohistochemistry (IHC) criteria. (B) Box plot analysis showing mRNA expression levels of *FZD6* in the different immunohistochemical subtypes. (C) Box plot analysis showing expression of *FZD6* in PAM50 subtypes [49]. (D–G) Box plot analyses of *WNT11* (D) *WNT5B* (E) *WNT1* (F) and *WNT3A* (G) expression in PAM50 subtypes. CN, copy number; LumA, luminal A; LumB, luminal B.

and stable RNA interference approaches. Depletion of FZD6 did not perturb the metabolism/proliferation of breast cancer cells, with the exception of the HCC1143 cell line (Figure 3A). Cell cycle profiles and sub-G_1 DNA content were unchanged, suggesting that cell proliferation and apoptosis are not modified in the absence of the receptor (data not shown). In contrast, there was a significant reduction in invasive potential after depletion of FZD6. The inhibitory effect of the small interfering RNAs (siRNAs) was proportional to the level of FZD6 knockdown, and the oligonucleotides were unable to modify the invasive potential of MDA-MB-436 cells with no membrane expression of FZD6, which should rule out potential off-target effects of the siRNAs (Figure 3B). The chosen siRNAs were confirmed to cause strong knockdown of *FZD6* mRNA expression (supplementary material, Figure S4B). Verification of surface depletion of FZD6 protein in the MD-MB-231 cell line by ImageStream analysis is shown in supplementary material, Figure S4C. These results were further validated with the MDA-MB-231 cell lines with permanent FZD6 knockdown caused by shRNAs (Figure 3A, B).

Organoid 3D cultures in Matrigel have been used to determine the degree of transformation of breast cancer cells [34]. In the absence of FZD6, the symmetrical shape of breast cancer acini forming in the Matrigel structure was significantly increased (supplementary

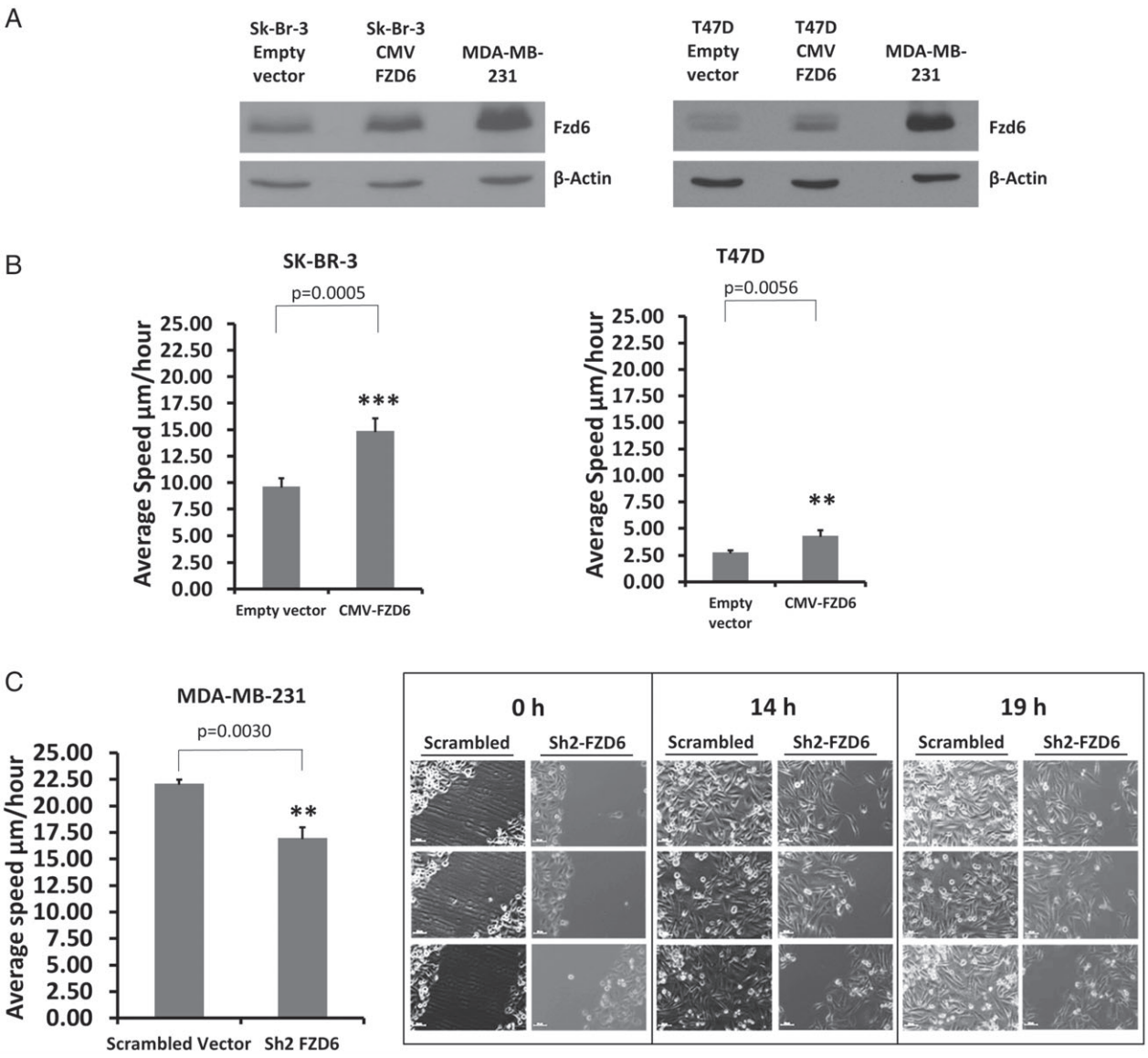

Figure 2. Cell motility assays. (A) Western blot analysis showing FZD6 protein levels in SK-BR-3 and T47D breast cancer cell lines following transient transfection of CMV-*FZD6* or CMV-control expression vectors. MDA-MB-231 cell lysates were used as a positive FZD6 control. (B) Cells were placed in a live imaging system and filmed for 24 h. The motility of green fluorescent protein-positive (i.e. transfected) cells was calculated, and is plotted on the *y*-axis. (C) MDA-MB-231 cells infected with lentiviruses containing control (scrambled) or *FZD6* (Sh2) shRNA were grown as a monolayer, and then scratched with a pipette tip. Pictures were taken at the indicated times, and show the closure of the wound in control (scrambled) but not in *FZD6*-downregulated (Sh2-*FZD6*) cells. Quantification of the experiment is shown in the bar plot. Error bars indicate SEs, and asterisks indicate statistical significance (Student's *t*-test).

material, Figure S5A–D). This experiment indicates that the increased expression of the receptor in cancer induces disorganized 3D growth, promoting a more aggressive phenotype. Notably, forced expression of *FZD6* in non-transformed MCF10A mammary epithelial cells modified 3D growth, inducing larger and less circular acini, validating the hypothesis that the receptor is a mammary protooncogene (Figure S5E–G). *FZD6* overexpression in MCF10A cells was confirmed by RT-qPCR (supplementary material, Figure S4D).

FZD6 regulates the metastatic process *in vivo*

To assess the role of FZD6 in growth and metastasis of breast cancer cells *in vivo*, we transplanted highly metastatic MDA-MB-231 cells into the mammary fat pads of immunocompromised NSG mice. In this model, breast cancer cells invade different organs, including the lungs, liver, heart, and bones, which are also sites for metastasis in humans. Despite the fact that growth of FZD6-negative cells was slightly delayed in comparison with control cells, at the end of the experiment the size of the primary tumour masses was similar in the two groups, indicating that FZD6 is largely dispensable for breast cancer cell proliferation *in vivo* (Figure 4A). However, there was a clear difference in the metastatic patterns. Specifically, we detected significantly fewer mice with bone metastases and a non-significant reduction in mice with heart and liver metastases when they were injected with FZD6-depleted cells with respect to

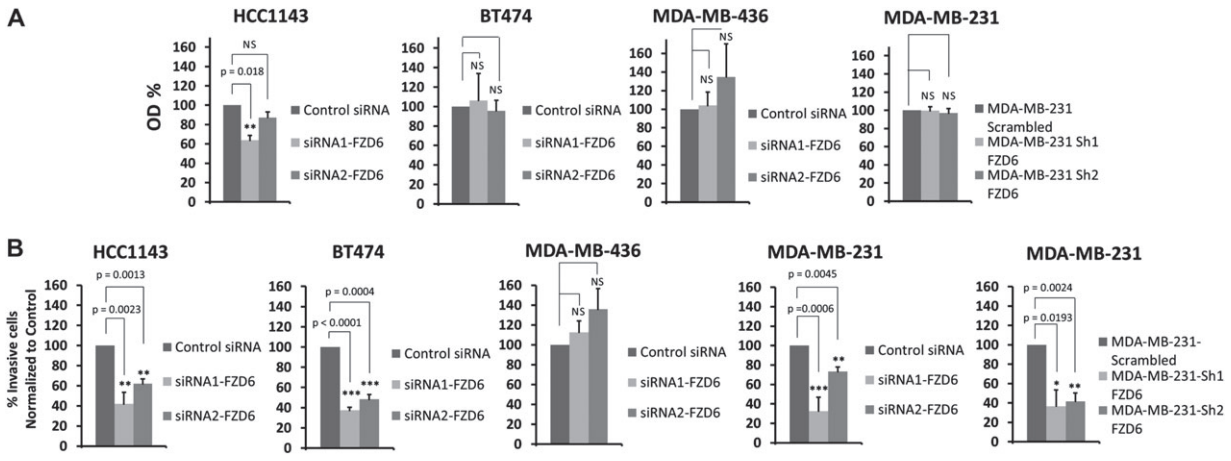

Figure 3. Effects of siRNA or shRNA *FZD6* knockdown in breast cancer cell lines. (A) MTS assay showing the metabolic activity, expressed as optical density (OD) units, of the different breast cancer cell lines in the presence of control or *FZD6* siRNAs. MDA-MB-231 cells were stably transfected with control (scrambled) or *FZD6* shRNAs (Sh1 and Sh2). Error bars indicate SEs, and asterisks indicate statistical significance (Student's *t*-test, $n = 3$). (B) *In vitro* invasion assays of the breast cancer cell lines transfected as described in (A). Error bars indicate SEs, and asterisks indicate statistical significance (Student's *t*-test, $n = 3$). NS, not significant.

control cell-injected mice (Figure 4B; supplementary material, Table S3A). The difference in metastatic growth in the liver has been further highlighted by the use of a score system that takes into account the number and size of metastases (supplementary material, Table S3B). Immunohistochemical analysis showed that FZD6 expression was reactivated in all metastases originating from cells infected with the *FZD6* shRNA-targeting retrovirus, probably because of silencing or loss of the shRNA vector in the absence of selective pressure (an example is shown in supplementary material, Figure S6A). This should explain why the difference in metastatic potential between FZD6-expressing and FZD6-non-expressing cells appeared to be attenuated *in vivo* as compared with the *in vitro* assays. Overall, these results support the hypothesis that FZD6 is dispensable for proliferation, but is required for motility, invasion and organ tropism of TNBC cells.

FZD6 signalling regulates fibronectin deposition and assembly of the actin cytoskeleton in MDA-MB-231 cells

We next investigated whether FZD6 could be involved in the regulation of the extracellular matrix, and fibronectin in particular. Different studies have demonstrated that the Wnt–planar cell polarity non-canonical pathway is essential for deposition of the extracellular matrix and organization of fibrillar fibronectin during frog gastrulation [35,36]. It has also been shown that growth factors such as epidermal growth factor (EGF) induce motility and invasion by regulating the assembly of fibronectin at the surfaces of MDA-MB-231 breast cancer cells [37]. We were thus interested in determining whether FZD6 could regulate MDA-MB-231 cell invasion via reorganization of the fibronectin matrix. To this end, we quantified fibronectin in FZD6-positive and FZD6-negative cells. Detection of fibronectin by immunofluorescence analysis showed that there was a reduction in the number of fibronectin fibres after FZD6 knockdown (Figure 5A, B). By using confocal microscopy, we ascertained that fibronectin was dispersed in control cells, whereas it was concentrated in dots or blobs similar to endosomes in FZD6-depleted cells (Figure 5C). Extracellular polymerization of fibronectin can inhibit the assembly of stress fibres formed by F-actin inside the cell [38]. Furthermore, it has been shown that inhibition of FZD7 and FZD4 signalling promotes cell spreading and stress fibre formation [39]. In the absence of FZD6, F-actin is organized in long fibres running throughout the cell. In contrast, in control cells F-actin fibres are thinner and concentrated in discrete areas in the proximity of the plasma membrane (Figure 5C). Exogenous delivery of fibronectin rescues the actin phenotype, indicating that a functional pathway exists linking FZD6 signalling to fibronectin and actin (Figure 5D). To determine whether FZD6 controls invasion by regulating fibronectin deposition, we plated FZD6 wild-type and knockout cell lines in invasion chambers, and used EGF as a chemoattractant. Notably, exogenous supplementation of fibronectin partially restored the invasive potential of FDZ6-depleted cells (Figure 5E), demonstrating that there is a mechanistic link connecting FZD6 signalling to fibronectin and metastatic activity. It has been reported that frizzled receptors modulate the actin cytoskeleton via activation of the non-canonical pathway and Rho signalling in ovarian cancer cells [40]. Indeed, there was less active Rho in FZD6-depleted cells, suggesting that FZD6 modulates the actin cytoskeleton via non-canonical Wnt signalling (Figure 5F, G). Finally, we carried out a pathway over-representation analysis in the KCL cohort. This identified over-represented GO terms such as cytoskeletal organization, intermediate filament-based processes and cell polarity within the 200 most *FZD6*-coexpressed genes, further supporting our hypothesis that a major function of FZD6 signalling

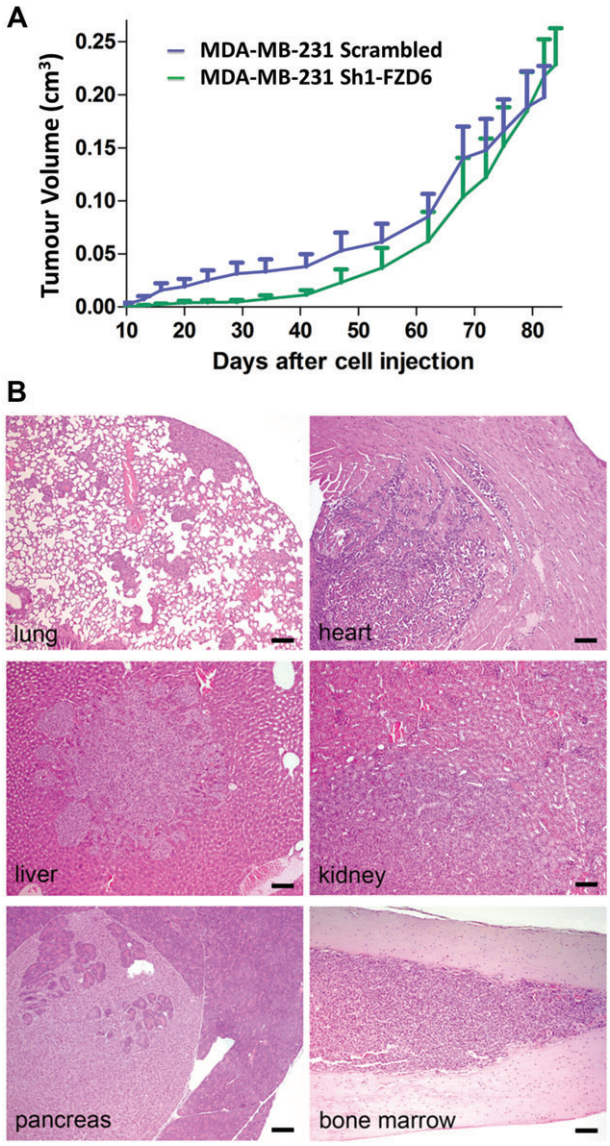

Figure 4. Orthotopic xenotransplantation of MB-MDA-231 cells with or without FZD6 expression in NSG mice. (A) MB-MDA-231 cells infected with a lentivirus containing *FZD6* (Sh1) or control (scrambled) shRNAs were injected into the fat pads of immunocompromised NSG mice. Growth of the primary tumour was measured two times per week with callipers. Error bars indicate SEs. (B) H&E staining of representative sections showing metastatic dissemination. Scale bars: 100 µm.

is to regulate cancer cell structure and movements (supplementary material, Figure S6B).

Prognostic significance of FZD6 expression in breast cancer patients

We carried out immunohistochemical analysis with an FZD6 antibody in a retrospective Italian cohort of 352 patients with node-negative early breast cancer (T1–T2, NO) (supplementary material, Table S1). Cytoplasmic and membranous staining was present in 20.2% of the specimens (Figure 6A–D). When we considered the whole patient cohort, FZD6 expression was not significantly associated with clinical features (supplementary material, Table S4). However, Kaplan–Meier analysis indicated that FZD6 expression was significantly associated with reduced distant relapse-free survival (DRFS) in the TNBC patient subgroup, whereas there was no significant association with other subtypes (Figure 6E and data not shown). In multivariate analysis, FZD6 expression was an independent prognostic indicator for DFS and DRFS in triple-negative cases [respectively: hazard ratio (HR) 5.7, 95% confidence interval (CI) 1.5–22.9, $p = 0.011$; and HR 6.8, 95% CI 1.2–37.4, $p = 0.027$] (supplementary material, Table S5). Tumour grade was the only independent factor influencing DFS and DRFS in the whole patient population (supplementary material, Table S6). The prognostic value of *FZD6* expression was investigated at the mRNA level with the aid of an online survival analysis tool to rapidly assess the effect of gene expression on breast cancer prognosis [41]. Consistent with the immunohistochemical analysis, high *FZD6* expression in tumours from lymph node-negative TNBC patients predicts a significant risk of distant metastatic recurrence (HR 2.35, 95% CI 1.16-4.75, $p = 0.014$) (Figure 6F).

Discussion

At least four main molecular subclasses of breast cancer have been identified so far: luminal A, luminal B, HER2-positive, and basal-like, which largely overlaps with the clinically defined TNBC forms. These show significant differences in incidence, survival, and response to therapy [42]. Accurate molecular phenotyping of breast cancer is thought to be key for the identification of patient groups in need of more specific, personalized care.

In this study, we assessed expression of *FZD6* in public databases, a cohort of breast cancer cases enriched for the TNBC subtype collected in Guy's Hospital, and a retrospective Italian cohort of 352 patients with node-negative early breast cancer (classified as T1–T2, N0). The main finding of this analysis is that the genomic region encompassing *FZD6*, but not other frizzled receptors, is amplified with high frequency in breast cancer. We have also observed an increased incidence of *FZD6* gains and augmented gene expression in triple-negative cases. However, other cancer subtypes, such as ER-positive breast cancers, show amplification and overexpression of *FZD6* in the analysed databases. Gene amplification is almost certainly one driver of high expression of *FZD6* in breast cancer. In multivariate analysis, expression of FZD6 protein was significantly associated with lower metastasis-free survival in patients with TNBC.

Previous studies have highlighted the important role of Wnt signalling in breast cancer. Wnt ligands such as WNT5A, WNT11 and WNT3A have been shown to promote migration and invasion of breast cancer cell lines *in vitro* and *in vivo* [43–45]. MB-MDA-231 cell line xenografts overexpressing secreted Frizzled-related protein 1, a Wnt pathway inhibitor, produced fewer

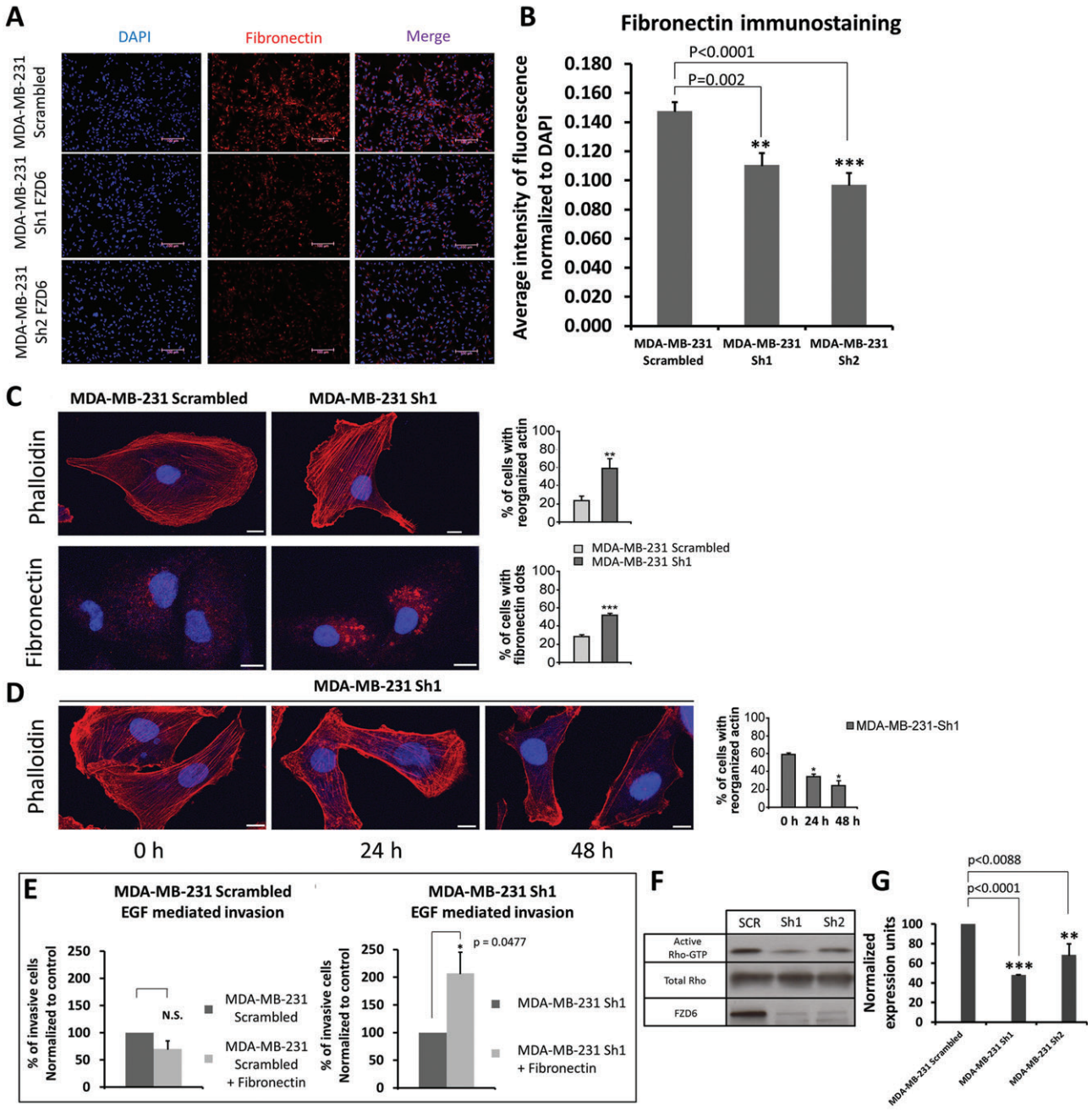

Figure 5. The actin cytoskeleton and fibronectin matrix are rearranged in the absence of FZD6, and exogenous fibronectin rescues the actin phenotype and invasive potential of MDA-MB-231 cells. (A) Images showing expression of the fibronectin matrix (red) in the control (scrambled) or FZD6-depleted (Sh1 and Sh2) cell lines. Nuclei were stained with 4′,6-diamidino-2-phenylindole (DAPI) (blue). (B) Quantification of the experiment shown in (A). The fibronectin fluorescence relative to DAPI was quantified with imaging software. Error bars indicate SEs, and asterisks indicate statistical significance (student's *t*-test). (C) Assembly of F-actin fibres in control (scrambled) or FZD6-depleted MDA-MB-231 (Sh1) cells was detected by confocal microscopy with phalloidin, to visualize actin, and DRAQ5, to visualize nuclei. Fibronectin was also assessed by confocal microscopy and two phenotypes were noted: dispersed in control cells, and dots/blobs in the absence of FZD6 expression. Bar plots on the right side of the panel show quantification of the fibronectin and actin changes. (D) FZD6-depleted MDA-MB-231 cells were exposed to exogenous fibronectin for the indicated times, and subjected to confocal analysis to detect the actin cytoskeleton. Quantification is shown in the bar plot. Confocal data are expressed as percentages of total, as means ± SEs of three independent experiments, with at least 100 cells quantified per experiment. $^{***}p < 0.01$, $^{**}p < 0.01$ and $^{*}p < 0.05$ as compared with control untreated cells (Student's *t*-test). (E) *In vitro* invasion assay showing rescue of EGF-mediated invasion in FZD6-depleted (Sh1) but not in control (scrambled) MDA-MB231 cell lines exposed to exogenous fibronectin. Error bars indicate SEs, and the asterisk indicates statistical significance ($p = 0.0477$, Student's *t*-test). (F) GST pull-down/western blot analysis to detect active forms of Rho in MDA-MB-231 cells infected with control (SCR) or *FZD6* (Sh1 and Sh2) shRNAs. Western blotting was carried out with antibodies recognizing FZD6 or Rho proteins, as indicated. (G) Densitometric quantification of active Rho in three independent pull-down experiments as shown in (F). Error bars indicate average values ± standard error of the mean (SEM), and asterisks indicate statistical significance ($^{***}p < 0.0001$, $^{**}p < 0.0088$, Student's *t*-test).

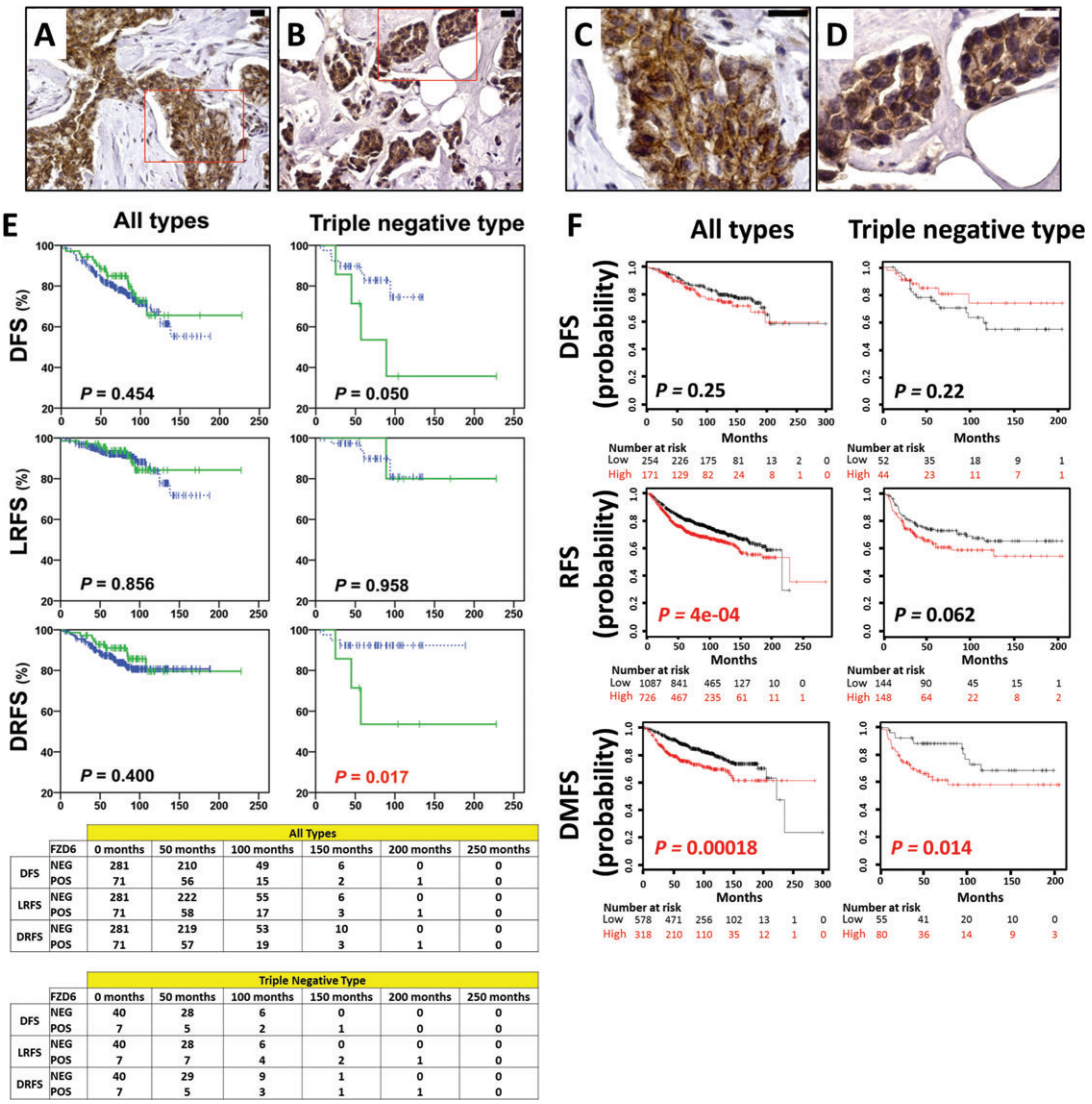

All Types	FZD6	0 months	50 months	100 months	150 months	200 months	250 months
DFS	NEG	281	210	49	6	0	0
	POS	71	56	15	2	1	0
LRFS	NEG	281	222	55	6	0	0
	POS	71	58	17	3	1	0
DRFS	NEG	281	219	53	10	0	0
	POS	71	57	19	3	1	0

Triple Negative Type	FZD6	0 months	50 months	100 months	150 months	200 months	250 months
DFS	NEG	40	28	6	0	0	0
	POS	7	5	2	1	0	0
LRFS	NEG	40	28	6	0	0	0
	POS	7	7	4	2	1	0
DRFS	NEG	40	29	9	1	0	0
	POS	7	5	3	1	1	0

Figure 6. FZD6 protein expression in breast cancer biopsies predicts distant metastasis. (A, B) Immunohistochemical analysis showing membranous expression of FZD6 in two invasive human TNBCs. (C, D) Enlargement of the areas indicated by red squares in (A) and (B), respectively, showing FZD6-positive tumour cells invading a vessel and infiltrating the fibroadipose tissue. Scale bars: 20 µm. (E) Kaplan–Meier estimates of DFS, local relapse-free survival (LRFS) and DRFS in breast cancer cases from the Italian cohort with (green solid line) or without (blue dashed line) expression of FZD6 in the cell membrane as assessed by immunohistochemistry. Statistical significance was assessed with the log-rank test. Numbers at risk are indicated in the table in the bottom of the panel. (F) Graphs were obtained with the Kaplan–Meier plotter (kmplotter.com) selecting lymph node-negative patients and the autoselect best cut-off option. Red lines indicate high *FZD6* expression, and black lines indicate low *FZD6* expression. Statistical significance was assessed with the log-rank test.

metastases in mice than injection with the control cell line [43]. *FZD7* knockdown reduces canonical Wnt signalling, tumour cell proliferation and invasiveness in breast cancer *in vivo* [12]. Klemm *et al* suggested a role of the β-catenin-independent pathway in breast cancer brain metastases, and observed substantial increases in cell invasiveness in the MB-MDA-231 and MCF7 cell lines after stimulation with WNT5A and WNT5B, without observing β-catenin activation [46]. Furthermore, Sottnik *et al* have highlighted the important role of Wnt signalling in bone metastasis, in keeping with our own observation of reduced bone metastasis in mice injected with FZD6-depleted MDA-MB-231 cells [47]. The therapeutic value of eliminating even small percentages of aggressive cancer clones should not be underestimated, as demonstrated in the MMTV-PyMT model of breast cancer, in which knockdown of keratin 14 blocked collective invasion *in vitro* and *in vivo*, despite the fact that only 2% of tumour cells expressed this marker [48]. There is increasing interest in the importance of cell invasion, motility and reseeding of metastases even after initial tumour cell dissemination.

Our study corroborates the view that components of the Wnt/β-catenin-independent signalling pathway have a key role in regulating cell movement, invasion and metastasis in breast cancer, opening new diagnostic and therapeutic opportunities. First, positivity for FZD6 might be used to identify patients with TNBC with a higher risk of metastatic recurrence who would benefit from an aggressive therapeutic approach. Second, surface expression of FZD6 could be used to develop naked or toxin-conjugated therapeutic antibodies to

target the aggressive breast cancer cell subclones that are the leaders of collective invasion.

Author contributions statement

The authors contributed in the following way: GC: carried out experiments, analysed data, and wrote the paper; RL, MP: carried out patient immunohistochemical analysis and analysed clinical data; GS, MI, AL, DB VDL: analysed data and carried out the *in vivo* work; MS, GF: carried out confocal analyses; SE, ES: established 3D breast cultures; HY, RFN: provided primary and established breast cell lines, and helped with the interpretation of the results; PV: contributed to the cell motility assays; MM, PGN, LP: provided patient material; HM, JQ, AG, PM, ANT: provided breast cancer patient databases and carried out bioinformatics analyses; MP, SI, VDL: analysed data and wrote sections of the paper; AS conceived the study, analysed data, and wrote the manuscript.

Acknowledgements

This work was funded in part by the Italian Association of Cancer Research (IG15196 to VDL, and IG11652 to MS), Mediapharma srl (to GS and SI), Breakthrough Breast Cancer (recently merged with Breast Cancer Campaign forming Breast Cancer Now) (to ANT, HM, and AG), and Brunel University (to AS). GS and SI were supported by Ministero Finalizzata 2011/2012.

References

1. Botha JL, Bray F, Sankila R, *et al.* Breast cancer incidence and mortality trends in 16 European countries. *Eur J Cancer* 2003; **39:** 1718–1729.
2. Cianfrocca M, Goldstein LJ. Prognostic and predictive factors in early-stage breast cancer. *Oncologist* 2004; **9:** 606–616.
3. Peto R, Boreham J, Clarke M, *et al.* UK and USA breast cancer deaths down 25% in year 2000 at ages 20–69 years. *Lancet* 2000; **355:** 1822.
4. Early Breast Cancer Trialists' Collaborative Group (EBCTCG). Effects of chemotherapy and hormonal therapy for early breast cancer on recurrence and 15-year survival: an overview of the randomised trials. *Lancet* 2005; **365:** 1687–1717.
5. Eifel P, Axelson JA, Costa J, *et al.* National Institutes of Health Consensus Development Conference Statement: adjuvant therapy for breast cancer, November 1–3, 2000. *J Natl Cancer Inst* 2001; **93:** 979–989.
6. Goldhirsch A, Glick JH, Gelber RD, *et al.* Meeting highlights: international expert consensus on the primary therapy of early breast cancer 2005. *Ann Oncol* 2005; **16:** 1569–1583.
7. Reya T, Clevers H. Wnt signalling in stem cells and cancer. *Nature* 2005; **434:** 843–850.
8. Lyuksyutova AI, Lu CC, Milanesio N, *et al.* Anterior–posterior guidance of commissural axons by Wnt-frizzled signaling. *Science* 2003; **302:** 1984–1988.
9. Fischer T, Guimera J, Wurst W, *et al.* Distinct but redundant expression of the Frizzled Wnt receptor genes at signaling centers of the developing mouse brain. *Neuroscience* 2007; **147:** 693–711.
10. Malanchi I, Santamaria-Martinez A, Susanto E, *et al.* Interactions between cancer stem cells and their niche govern metastatic colonization. *Nature* 2012; **481:** 85–89.
11. Valastyan S, Reinhardt F, Benaich N, *et al.* A pleiotropically acting microRNA, miR-31, inhibits breast cancer metastasis. *Cell* 2009; **137:** 1032–1046.
12. Yang L, Wu X, Wang Y, *et al.* FZD7 has a critical role in cell proliferation in triple negative breast cancer. *Oncogene* 2011; **30:** 4437–4446.
13. Gujral TS, Chan M, Peshkin L, *et al.* A noncanonical Frizzled2 pathway regulates epithelial–mesenchymal transition and metastasis. *Cell* 2014; **159:** 844–856.
14. Saramaki OR, Porkka KP, Vessella RL, *et al.* Genetic aberrations in prostate cancer by microarray analysis. *In J Cancer* 2006; **119:** 1322–1329.
15. Vincan E, Barker N. The upstream components of the Wnt signalling pathway in the dynamic EMT and MET associated with colorectal cancer progression. *Clin Exp Metastasis* 2008; **25:** 657–663.
16. Wu QL, Zierold C, Ranheim EA. Dysregulation of Frizzled 6 is a critical component of B-cell leukemogenesis in a mouse model of chronic lymphocytic leukemia. *Blood* 2009; **113:** 3031–3039.
17. Bengochea A, de Souza MM, Lefrancois L, *et al.* Common dysregulation of Wnt/Frizzled receptor elements in human hepatocellular carcinoma. *Br J Cancer* 2008; **99:** 143–150.
18. Cantilena S, Pastorino F, Pezzolo A, *et al.* Frizzled receptor 6 marks rare, highly tumourigenic stem-like cells in mouse and human neuroblastomas. *Oncotarget* 2011; **2:** 976–983.
19. Yasaei H, Gilham E, Pickles JC, *et al.* Carcinogen-specific mutational and epigenetic alterations in INK4A, INK4B and p53 tumour-suppressor genes drive induced senescence bypass in normal diploid mammalian cells. *Oncogene* 2013; **32:** 171–179.
20. Kamburov A, Pentchev K, Galicka H, *et al.* ConsensusPathDB: toward a more complete picture of cell biology. *Nucleic Acids Res* 2011; **39:** D712–D717.
21. Kamburov A, Wierling C, Lehrach H, *et al.* ConsensusPathDB – a database for integrating human functional interaction networks. *Nucleic Acids Res* 2009; **37:** D623–D628.
22. Binns D, Dimmer E, Huntley R, *et al.* QuickGO: a web-based tool for Gene Ontology searching. *Bioinformatics* 2009; **25:** 3045–3046.
23. Bauer DF. Constructing confidence sets using rank statistics. *J Am Stat Assoc* 1972; **67:** 687–690.
24. Santilli G, Cervellera MN, Johnson TK, *et al.* PARP co-activates B-MYB through enhanced phosphorylation at cyclin/cdk2 sites. *Oncogene* 2001; **20:** 8167–8174.
25. Gazinska P, Grigoriadis A, Brown JP, *et al.* Comparison of basal-like triple-negative breast cancer defined by morphology, immunohistochemistry and transcriptional profiles. *Mod Pathol* 2013; **26:** 955–966.
26. Watkins J, Weekes D, Shah V, *et al.* Genomic complexity profiling reveals that HORMAD1 overexpression contributes to homologous recombination deficiency in triple-negative breast cancers. *Cancer Discov* 2015; **5:** 488–505.
27. de Rinaldis E, Gazinska P, Mera A, *et al.* Integrated genomic analysis of triple-negative breast cancers reveals novel microRNAs associated with clinical and molecular phenotypes and sheds light on the pathways they control. *BMC Genomics* 2013; **14:** 643.
28. Lattanzio R, Marchisio M, La Sorda R, *et al.* Overexpression of activated phospholipase Cgamma1 is a risk factor for distant metastases in T1–T2, N0 breast cancer patients undergoing adjuvant chemotherapy. *Int J Cancer* 2013; **132:** 1022–1031.
29. Lattanzio R, Ghasemi R, Brancati F, *et al.* Membranous Nectin-4 expression is a risk factor for distant relapse of T1–T2, N0 luminal-A early breast cancer. *Oncogenesis* 2014; **3:** e118.
30. Goldhirsch A, Winer EP, Coates AS, *et al.* Personalizing the treatment of women with early breast cancer: highlights of the St Gallen

International Expert Consensus on the Primary Therapy of Early Breast Cancer 2013. *Ann Oncol* 2013; **24:** 2206–2223.
31. Cheang MC, Chia SK, Voduc D, *et al.* Ki67 index, HER2 status, and prognosis of patients with luminal B breast cancer. *J Natl Cancer Inst* 2009; **101:** 736–750.
32. Forbes SA, Beare D, Gunasekaran P, *et al.* COSMIC: exploring the world's knowledge of somatic mutations in human cancer. *Nucleic Acids Res* 2015; **43:** D805–D811.
33. Curtis C, Shah SP, Chin SF, *et al.* The genomic and transcriptomic architecture of 2,000 breast tumours reveals novel subgroups. *Nature* 2012; **486:** 346–352.
34. Marchese S, Silva E. Disruption of 3D MCF-12A breast cell cultures by estrogens – an in vitro model for ER-mediated changes indicative of hormonal carcinogenesis. *PLoS One* 2012; **7:** e45767.
35. Dzamba BJ, Jakab KR, Marsden M, *et al.* Cadherin adhesion, tissue tension, and noncanonical Wnt signaling regulate fibronectin matrix organization. *Dev Cell* 2009; **16:** 421–432.
36. Goto T, Davidson L, Asashima M, *et al.* Planar cell polarity genes regulate polarized extracellular matrix deposition during frog gastrulation. *Curr Biol* 2005; **15:** 787–793.
37. Boscher C, Nabi IR. Galectin-3- and phospho-caveolin-1-dependent outside-in integrin signaling mediates the EGF motogenic response in mammary cancer cells. *Mol Biol Cell* 2013; **24:** 2134–2145.
38. Shi F, Long X, Hendershot A, *et al.* Fibronectin matrix polymerization regulates smooth muscle cell phenotype through a Rac1 dependent mechanism. *PLoS One* 2014; **9:** e94988.
39. Dufourcq P, Leroux L, Ezan J, *et al.* Regulation of endothelial cell cytoskeletal reorganization by a secreted frizzled-related protein-1 and frizzled 4- and frizzled 7-dependent pathway: role in neovessel formation. *Am J Pathol* 2008; **172:** 37–49.
40. Asad M, Wong MK, Tan TZ, *et al.* FZD7 drives in vitro aggressiveness in Stem-A subtype of ovarian cancer via regulation of non-canonical Wnt/PCP pathway. *Cell Death Dis* 2014; **5:** e1346.
41. Gyorffy B, Lanczky A, Eklund AC, *et al.* An online survival analysis tool to rapidly assess the effect of 22,277 genes on breast cancer prognosis using microarray data of 1,809 patients. *Breast Cancer Res Treat* 2010; **123:** 725–731.
42. Carey LA, Perou CM, Livasy CA, *et al.* Race, breast cancer subtypes, and survival in the Carolina Breast Cancer Study. *JAMA* 2006; **295:** 2492–2502.
43. Matsuda Y, Schlange T, Oakeley EJ, *et al.* WNT signaling enhances breast cancer cell motility and blockade of the WNT pathway by sFRP1 suppresses MDA-MB-231 xenograft growth. *Breast Cancer Res* 2009; **11:** R32.
44. Zhu Y, Tian Y, Du J, *et al.* Dvl2-dependent activation of Daam1 and RhoA regulates Wnt5a-induced breast cancer cell migration. *PLoS One* 2012; **7:** e37823.
45. Pukrop T, Klemm F, Hagemann T, *et al.* Wnt 5a signaling is critical for macrophage-induced invasion of breast cancer cell lines. *Proc Natl Acad Sci USA* 2006; **103:** 5454–5459.
46. Klemm F, Bleckmann A, Siam L, *et al.* beta-catenin-independent WNT signaling in basal-like breast cancer and brain metastasis. *Carcinogenesis* 2011; **32:** 434–442.
47. Sottnik JL, Hall CL, Zhang J, *et al.* Wnt and Wnt inhibitors in bone metastasis. *Bonekey Rep* 2012; **1:** 101.
48. Cheung KJ, Gabrielson E, Werb Z, *et al.* Collective invasion in breast cancer requires a conserved basal epithelial program. *Cell* 2013; **155:** 1639–1651.
49. Parker JS, Mullins M, Cheang MCU, *et al.* Supervised risk predictor of breast cancer based on intrinsic subtypes. *J Clin Oncol* 2009; **27:** 1160–1167.

SUPPLEMENTARY MATERIAL ONLINE

Supplementary materials and methods

Supplementary figure legends

Figure S1. The diagram depicts the studies from which samples of the KCL cohort used in this study were derived.

Figure S2. Analysis of copy number alterations (CNA) and RNA expression of *FZD6*.

Figure S3. Expression of *FZD6* in breast cancer cell lines.

Figure S4. Expression of exogenous and endogenous *FZD6* and RNAi efficiency in breast cancer cell lines.

Figure S5. 3D cultures of transformed and non-transformed mammary cells.

Figure S6. Immunohistochemical analysis of tumours excised from mice injected with MDA-MB-231 cells and Gene Ontology (GO) enrichment analysis of top 200 *FZD6* coexpression genes.

Table S1. Patients and tumour characteristics (n = 352).

Table S2. Copy Number Variation (CNV) and overexpression of Frizzled (FZD) receptor 1 to 10 in primary breast cancer samples mined using the COSMIC repository (http://cancer.sanger.ac.uk/cancergenome/projects/cosmic/about).

Table S3. Assessment of metastatic growth in mice injected with MB-MDA-231 cells.

Table S4. FZD6 status according to clinicopathological features of patients.

Table S5. Multivariate analysis of FZD6 expression in triple negative tumours.

Table S6. Multivariate analysis of FZD6 expression in breast tumours.